inorganics

MDPI

Article

Copper(II) Halide Salts with 1-(4′-Pyridyl)-Pyridinediium

Jeffrey C. Monroe [1,*], Christopher P. Landee [2], Melanie Rademeyer [3] and Mark M. Turnbull [1,*]

1 Carlson School of Chemistry and Biochemistry, Clark University, 950 Main St., Worcester, MA 01610, USA
2 Department of Physics, Clark University, 950 Main St., Worcester, MA 01610, USA; clandee@clarku.edu
3 Department of Chemistry, University of Pretoria, Private Bag X20, Hatfield 0028, South Africa; Melanie.Rademeyer@up.ac.za
* Correspondence: jmonroe@clarku.edu (J.C.M.); mturnbull@clarku.edu (M.M.T.)

Received: 10 December 2019; Accepted: 24 February 2020; Published: 4 March 2020

Abstract: The compounds [1,4′-bipyridine]-1,1′-diium [$CuCl_4$] (**1**) and [1,4′-bipyridine]-1,1′-diium [$CuBr_4$] (**2**) were prepared and their crystal structures and magnetic properties are reported. The compounds are isomorphous and crystallize in the monoclinic space group *C*2/c. The cation crystallizes in a two-fold disordered fashion with the terminal nitrogen and carbon atoms exhibiting 50% occupancies. This results in a crystal packing arrangement with significant hydrogen bonding that is very similar to that observed in the corresponding 4,4′-bipyridinediium complexes. Temperature dependent magnetic susceptibility measurements and room temperature EPR spectroscopy indicate the presence of very weak antiferromagnetic exchange. The data were fit to the Curie–Weiss law and yielded Weiss constants of −0.26(5) K (**1**) and −1.0(1) K (**2**).

Keywords: Cu(II); magnetism; EPR; pyridine-based compound

1. Introduction

The importance of hydrogen bonding to crystal engineering has been noted in a number of recent studies [1–3]. The ability to predict or design an approximate packing structure using restricted avenues for strong hydrogen bonds is highly desirable in a variety of fields including crystal engineering [4], bioinorganic chemistry [5], and magnetism [6–9].

As described by Kumar et al. [10], the importance of the bifurcated $CuCl_2$···H–N hydrogen bond is considered with dications such as 4,4′-bipyridinediium, which form ABAB ribbons where A is the $CuCl_4$ dianion and B is the dication. A similar ribbon packing is observed for (4,4′-bipyridinediium)Cu_2X_6 (X = Cl, Br) [11]. The importance of the bifurcated $CuCl_2$···H–N hydrogen bond was also shown by Yahsi et al. [12] with a variety of boronic acid cations for crystal engineering. Given our previous work with pyridinium salts of tetrahalidocuprate ions [13–18], we were intrigued with the potential for observing and using such hydrogen bonding in the formation of low-dimensional lattices for magnetic study. In many tetrahalidocuprate compounds [13–24], the general formula may be written as $(BH)_2[CuX_4]$ where B is an organic base, most often an amine. The BH^+ moiety provides charge balance and influences the structure of the crystal lattice through its steric and electronic properties. Several complexes have been prepared using dibasic organic species resulting in complexes of the general formula $(BH_2)[CuX_4]$ [10,25–27].

Compounds with the doubly cationic [1,4′-bipyridine]-1,1′-diium are here described. While it was evident that the modification of the $(BH)_2[CuX_4]$ model to the $(BH)[CuX_4]$ scaffold could result in less well-isolated layers, chains, ladders or honeycombs, due to the loss of one bulky cation per CuX_4^{2-} unit, it was posited that some unique structures could be discovered, since the use of doubly cationic molecules is much less common. Thus, by exploring the use of [1,4′-bipyridine]-1,1′-diium (**B1H**), a sterically long, doubly cationic, and versatile counter-cation, it was proposed that design

features stemming from the directionality of the hydrogen bond donors would present themselves. The compounds [1,4′-bipyridine]-1,1′-diium [$CuCl_4$] (**1**), [1,4′-bipyridine]-1,1′-diium [$CuBr_4$] (**2**) are described here regarding the effect of hydrogen bonding on crystal packing and the effect of **B1H** as a design agent in the synthesis of magnetic materials.

2. Results and Discussion

2.1. Synthesis

The synthesis of **1** and **2** may be achieved directly in the appropriate concentrated acid solution with stoichiometric ratios of the starting materials. The synthetic method is summarized in Scheme 1 for **1** and **2**. Both compounds grow as flat plate crystals, with the expected colors for copper(II) halide salts (yellow, **1**; purple, **2**).

$$CuX_2 + (\mathbf{B1H})X_2 \xrightarrow{>3M\ HX} (\mathbf{B1H})[CuX_4]$$

Scheme 1. The preparation of **1** and **2** where **B1H** = [1,4′-bipyridine]-1,1′-diium and X = Cl, Br.

2.2. Structure

1 and **2** are isostructural with very similar lattice parameters, as shown in Table 1. Thus, in the following treatment, **2** is considered explicitly (Corresponding figures for **1** are shown in the Supplementary Materials as Figures S1 and S2).

Table 1. Crystallographic information for **1** and **2**.

	1	**2**
Formula	$C_{10}H_{10}N_2Cl_4Cu$	$C_{10}H_{10}N_2Br_4Cu$
Molecular Weight	363.54	541.38
Crystal System	monoclinic	monoclinic
Space Group	*C*2/c	*C*2/c
a(Å)	15.6790(11)	16.0672(9)
b(Å)	7.4315(5)	7.5861(4)
c(Å)	12.0742(8)	12.5969(6)
α(°)	90	90
β(°)	108.270(3)	108.126(2)
γ(°)	90	90
V(Å^3)	1335.95(16)	1459.21(13)
Z	4	4
T(K)	150(2)	150(2)
ϱ_{calc} (g cm^{-1})	1.803	2.464
μ(mm^{-1})	2.411	12.429
λ(Å)	0.71073	0.71073
Index Ranges	$-28 \le h \le 28$	$-22 \le h \le 21$
	$-13 \le k \le 13$	$-10 \le k \le 10$
	$-21 \le l \le 21$	$-16 \le l \le 16$
Indep. Reflections [$I > 2\sigma(I)$]	3060	1473
Obs. reflections	4022	1856
Parameters	94	95
Goodness of fit	1.021	1.063
R [$I > 2\sigma(I)$]	0.0432	0.0363
R_w [$I > 2\sigma(I)$]	0.0893	0.0795
R (all reflections)	0.0641	0.0530
R_w (all reflections)	0.0983	0.0850

The asymmetric unit of **2** contains half of a $CuBr_4^{2-}$ unit and half of a disordered **B1H** dication. The molecular unit of **2** is shown in Figure 1; the CuX_4 distorted tetrahedra and full **B1H** dications

are generated by 2-fold rotation axes running though Cu1 and the central bond of the **B1H** dication. The CuX_4^{2-} unit in **2** may be comparably described as a flattened tetrahedron or a distorted square planar unit with a mean *trans* angle [28] in **1** = 144.9° and in **2** = 142.9° (the corresponding τ_4 parameters are 0.53 (**1**) and 0.50 (**2**) [29]. The Cu–X bond lengths are those expected for a CuX_4^{2-} unit [13–24]; selected bond lengths and angles are given in Table 2. The Jahn-Teller distortion characteristic of four-coordinate copper(II) compounds causes variation of the bond angles from purely tetrahedral. The very close similarity in the structures of **1** and **2** is easily seen in the overlay drawing (Figure S3).

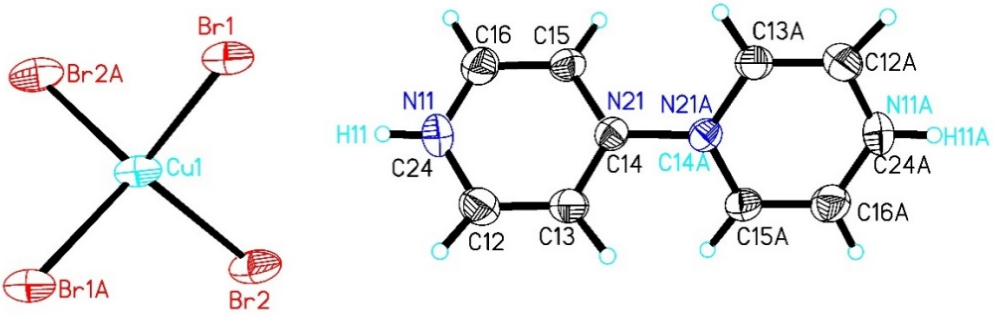

Figure 1. The molecular unit of **2**, shown as 50% probability thermal ellipsoids; hydrogen atoms are shown as spheres of arbitrary size. Disordered positions (N11/C24 and N21/C14) are labelled with both atom names. Symm. Op. A = $-x$, y, $-1/2 - z$.

Table 2. Selected bond lengths (Å) and angles (°) in **1** and **2**. (Symm. Op. a = −x, y, $\frac{1}{2}$ − z).

	1	**2**
Cu1–X1	2.2481(5)	2.3816(5)
Cu1–X2	2.2515(5)	2.3919(5)
X1–Cu1–X1a	140.63(3)	143.03(4)
X2–Cu1–X2a	145.24(3)	146.71(4)
X1–Cu1–X2	95.49(2)	95.231(19)
X1–Cu1–X2a	96.060(19)	95.190(18)
X1a–Cu1–X2	96.060(18)	95.189(18)
X1a–Cu1–X2a	95.49(2)	95.230(19)

The orientation of the organic group **B1H** is two-fold disordered in the lattice. Any given dication is hydrogen bonded to the $CuBr_4^{2-}$ unit via N11–H11. A superposition of the two orientations of the dication is shown in Figure 2 for **1**. Atoms N11/C24 and N21/C14 occupy identical positions in the lattice and each have 0.5 occupancy as required by symmetry. Atoms C12, C13, C15 and C16 are not disordered and have full occupancies. Labels A, B and C indicate symmetry generated atoms. The fact that the organic moiety is in fact disordered in the lattice indicates that the orientation must indeed be random; if the orientation were to alternate is some fashion, the crystals could exhibit a different space group and a larger unit cell to accommodate the additional symmetry.

The N11–H11/C24–H24 hydrogen bond donors from **B1H** are involved in a bifurcated hydrogen bond to X1 and X2, with parameters shown below in Table 3 and shown in Figure 3. The symmetry equivalent disordered C24–H24 hydrogen bonding parameters are identical; however, the hydrogen bonding strength is presumed to be much weaker due to the lower polarity of the C–H bond. The angle between the normals to the symmetry equivalent pyridine rings in **B1H** is 45.9° (**2**) (48.2°, **1**) as expected based on similar compounds [30–32]. Additional short C–H···Cl interactions are present in the structures (average $d_{C\cdots Cl}$~3.6 Å; average $\angle_{C-H\cdots Cl}$~149° for **1**). Complexes using **B1H** as the counterion have been previously reported including halido compounds of molybdenum and tungsten [31], the tetrachloridoplatinate and pentachloridostibnate salts [33] and a hexacyanidoferrate complex [34]. No structures involving tetrahedral metalate anions have been reported to our knowledge. The dihedral angles observed in the **B1H** cations are typically ~38° [30,31,33], significantly smaller than

observed here, but in the ferrate species [34] that angle is 44°, comparable to what is observed for **1** and **2**. None of the reported complexes exhibit the disorder observed for **1** and **2**.

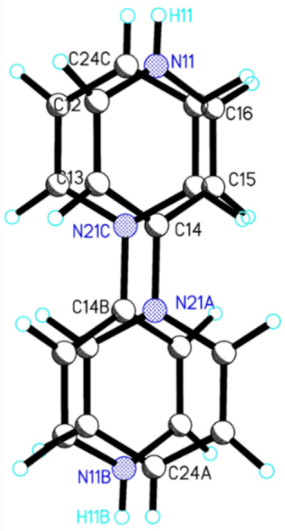

Figure 2. A superposition of the two disordered positions of the organic dication in **1**.

Table 3. Hydrogen bonding parameters in **1** and **2**.

DHA		DH (Å)	H···A (Å)	D···A (Å)	∢DHA (°)
N11–H11···X1	**1**	0.91(6)	2.47(6)	3.2699(18)	147(5)
	2	0.843(14)	2.66(3)	3.429(5)	152(4)
N11–H11···X2	**1**	0.91(6)	2.79(6)	3.464(2)	132(4)
	2	0.843(14)	2.99(4)	3.599(5)	131(4)

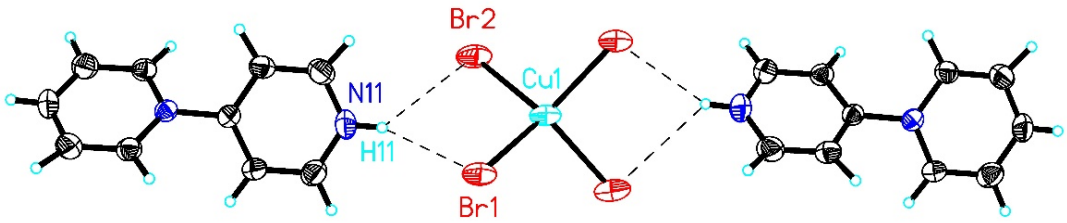

Figure 3. Br···H hydrogen bonding in **2**. See Table 3 for hydrogen bonding data.

The crystal packing is such that the $CuBr_4^{2-}$ and **B1H** dications alternate in three dimensions as shown in Figure 4a (Figure S2 for **1**). Due to the fact that there is only one **B1H** dication per $CuBr_4^{2-}$ unit, the $CuBr_4^{2-}$ units are close enough to each other to propagate weak magnetic interactions in three dimensions [**1** – $d_{Cl\cdots Cl}$ = 4.36 Å, $\measuredangle_{Cu\text{-}Cl\cdots Cl}$ = 119° and 109°, $\measuredangle_{Cu\text{–}Cl\cdots Cl\text{–}Cu}$ = 71°; **2** – $d_{Br\cdots Br}$ = 4.47 Å, $\measuredangle_{Cu\text{–}Br\cdots Br}$ = 120° and 108°, $\measuredangle_{Cu\text{–}Br\cdots Br\text{–}Cu}$ = 73°] [28]. It has been previously demonstrated in tetrahalidocuprate systems that the magnetic exchange is primarily dependent upon the halide···halide separation, rather than the distance between Cu(II) ions [35].

The crystal packing in **1** and **2** is very similar to that of (4,4′-bipyridinediium) $[CuCl_4]$ and 4,4′-(H_2diazastilbene) $[CuCl_4]$ [10], each of which are composed of the ABAB ribbons with bifurcated hydrogen bonds controlling the packing pattern. The limited directionality of the hydrogen bond donors controls the packing of these compounds, thus enabling control of the 3D structure.

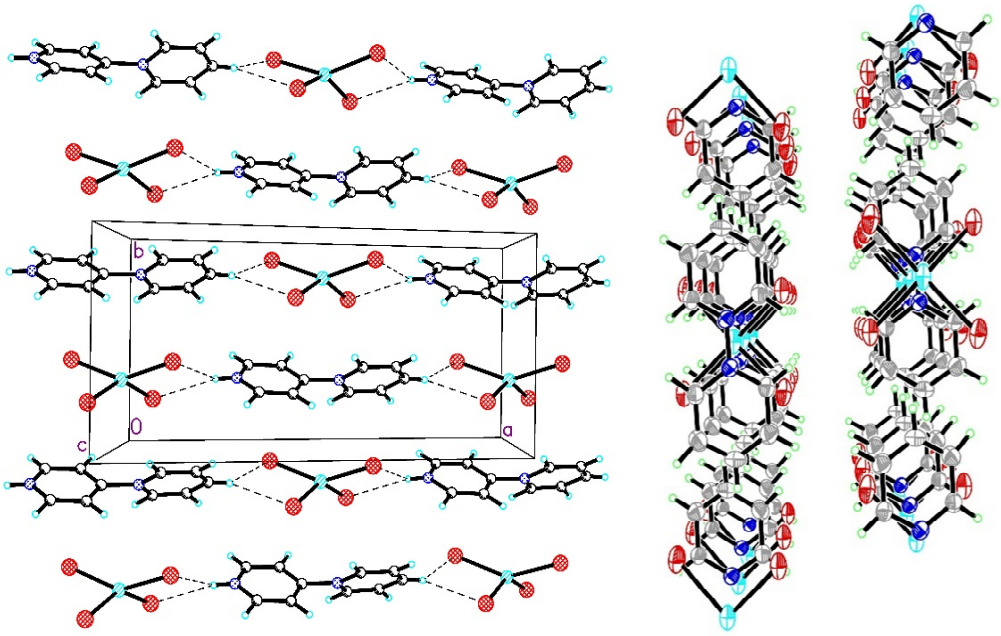

(**a**) (**b**)

Figure 4. (**a**) Packing of **B1H** and $CuBr_4$ units into a layer in **2**, viewed parallel to the *b*-axis. (**b**) Packing of layers in **2**, viewed parallel to the *c*-axis.

2.3. Magnetism

M(H) plots for **1** and **2** are shown in Figure 5. Comparison of the two plots indicates that the chloride analog exhibits weaker internal superexchange interactions as shown by the increased rate at which M(H) of **1** is nearing saturation at 50 kOe; **2** is still ~15% below saturation at that field. The internal interactions in compound **1** are sufficiently weak that the magnetization was ably fit to the Brillouin function, giving an average *g*-factor of 2.11.

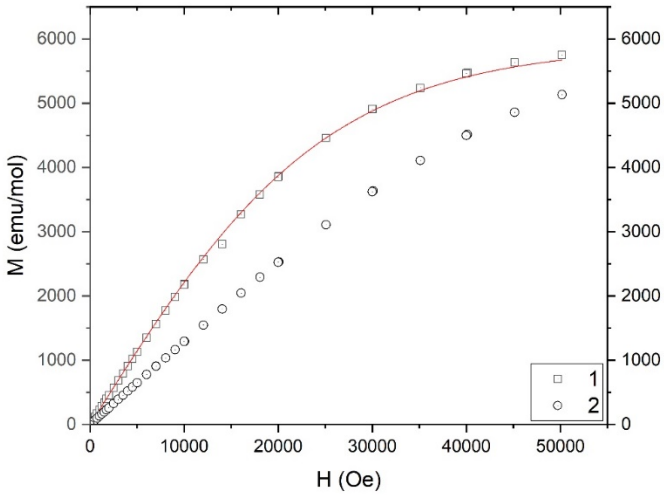

Figure 5. The magnetization of **1** (□) and **2** (○). The solid line is the fit to the S = $\frac{1}{2}$ Brillouin function.

The susceptibility versus temperature plots of **1** and **2** are void of structure and resemble the susceptibility of paramagnetic complexes. As demonstrated by the slight downturn in the χT(T) plots at low temperatures (Figure 6), there are very weak antiferromagnetic interactions. Given the weakness of the interactions, the 1/χ(T) data from 25 K to 310 K were fit to the Curie–Weiss model [36]. The fitted

parameters for **1** and **2** are shown in Table 4 and indicate very weak coupling as expected. Weaker coupling in the chloride than the bromide complex is observed as expected of two-halide pathways of isostructural pairs of this type [28] and as expected from the M(H) data (vide supra).

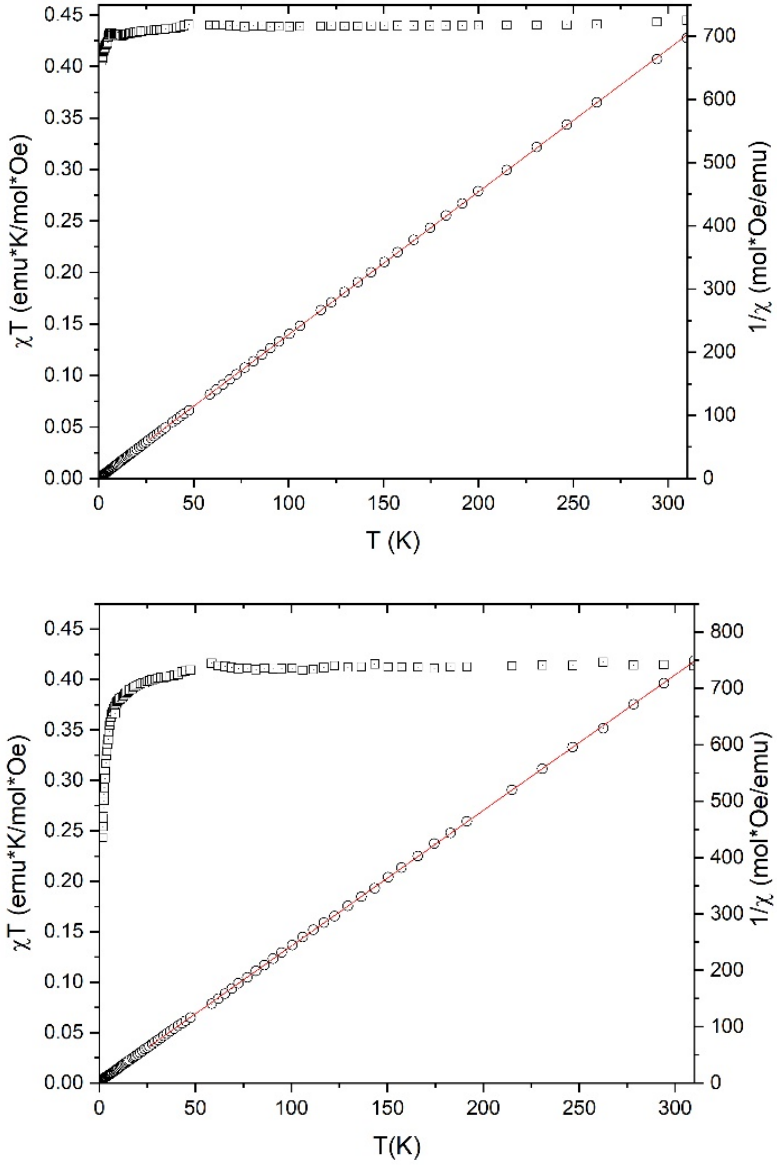

Figure 6. The magnetic susceptibility plotted as χT(T) (left axis) and 1/χ(T) (right axis) of **1** (top) and **2** (bottom).

Table 4. Fitted parameters to the Curie–Weiss Law for **1** and **2**. g_{ave} was calculated from the fitted value of the Curie constant (CC).

	CC (emu·K/mol·Oe)	θ (K)	g_{ave}	R^2
1	0.4406(1)	−0.26(5)	2.168	0.99999
2	0.4157(4)	−1.0(1)	2.105	0.99994

2.4. Powder X-Band EPR

Despite the very weak nature of superexchange in these complexes, no hyperfine structure is observed in the powder EPR spectra. Both compounds **1** and **2** display axial *g*-tensors with largely Lorentzian line shapes as determined by fits using EasySpin [37]. The powder spectra are shown

in Figure 7; the fitted *g*-values are g⊥ = 2.0594, g|| = 2.3363 (g_{ave} = 2.1517) (**1**) and g⊥ = 2.0820, g|| = 2.2361 (g_{ave} = 2.1334) (**2**). The broadening of g|| is much larger in **1** (G-strain = 0.0523) than in **2** (G-strain = 0.0064), both because Δg_e is larger and because the interactions are much weaker, such that the effect of collapsed hyperfine coupling on the linewidth is larger. The average *g*-factor from EPR studies is considered more accurate than that from the fits to the magnetization and 1/χ(T).

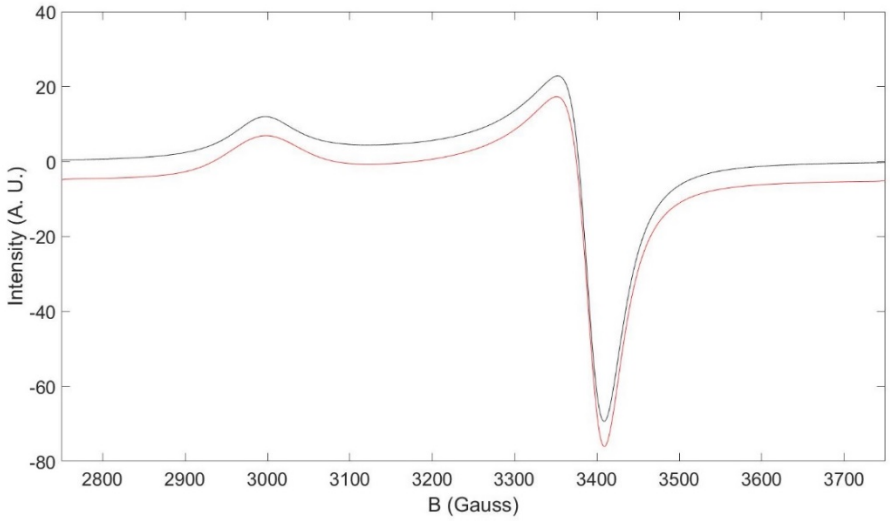

(**a**)

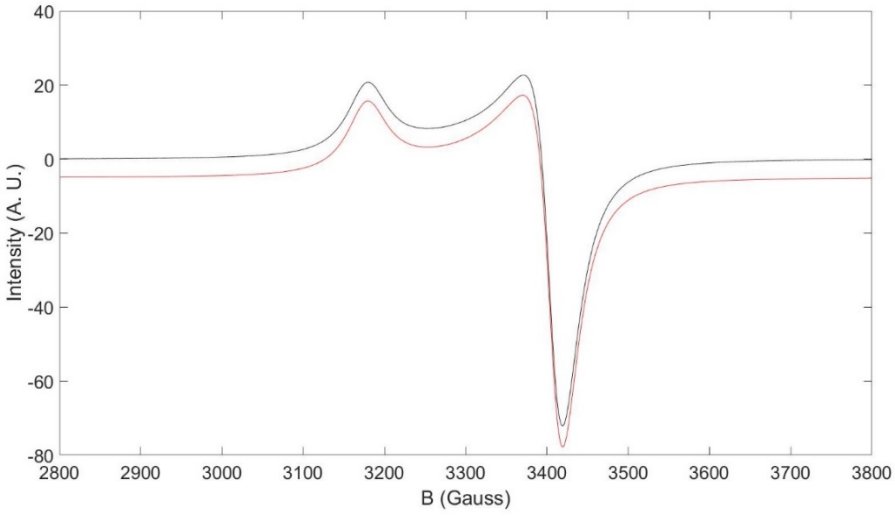

(**b**)

Figure 7. The X-band powder EPR spectra of **1** (**a**) and **2** (**b**) at room temperature with fits shown displaced from the data by −5 intensity units in red.

The average *g*-factor found from the fit to the Brillouin function agrees within 2% of that found from EPR studies, and that from 1/χ(T) is within about 1% for **1**. The average *g*-factor from the fit to 1/χ(T) for **2** is within 1.5% of that found from EPR studies. Similar to the findings of Farra et al. [38], g|| for the bromide salt is much smaller than that of the chloride salt and the g⊥ is much larger for the bromide salt compared to the chloride salt, most likely due to the spin orbit coupling and ligand field effects of the bromide ion versus the chloride ion [39].

3. Materials and Methods

[1,4′-bipyridine]-1,1′-diium dichloride x-hydrate was purchased from TCI and was used as received except for the synthesis of **2** for which a halide exchange (vide infra) was performed. Copper(II) chloride dihydrate was purchased from Allied Chemical Corp. and copper(II) bromide was purchased from Alfa Aesar and used without further purification. Powder X-ray diffraction data were collected with a Bruker D8 Focus diffractometer. IR spectra were obtained with a Perkin Elmer Spectrum 100 FT-IR spectrometer via ATR. Elemental analyses were performed at the Marine Science Institute, University of California-Santa Barbara, CA, USA.

3.1. Synthesis

[1,4′-Bipyridine]-1,1′-diium tetrachloridocuprate (**1**): $CuCl_2{\cdot}2H_2O$ (0.341 g, 2.00 mmol) was dissolved in ca. 5 mL H_2O, giving a blue solution. [1,4′-Bipyridine]-1,1′-diium dichloride *x*-hydrate (0.462 g, 2.02 mmol (calculation based on anhydrous form)) was dissolved in 5 mL H_2O and while stirring 15 drops of concentrated HCl were added to this solution. The [1,4′-bipyridine]-1,1′-diium dichloride solution was combined with the $CuCl_2$ solution giving a green solution. The solution was stirred for 5 more minutes and then left at room temperature, covered with filter paper. The following week, a mixture of blue and yellow crystals was isolated via vacuum filtration. The blue crystals were identified as $[Cu(B1)_2Cl_2](Cl)_2$ (B1 = 1-(4′-pyridyl)pyridinium) [40]. The filtrate was acidified with additional drops of concentrated HCl. One month later, yellow crystals of **1** were isolated from the solution via vacuum filtration, washed with H_2O and dried mechanically (0.3513 g, 48%). IR (cm^{-1}) 3043 (mult, m), 1634 (w, sh), 1615 (s), 1528 (w), 1505 (w), 1488 (w), 1474 (s), 1355 (w), 1280 (w), 1002 (w), 806 (s), 771 (s), 760 (m, sh), 718 (s), 670 (vs), 550 (w). CHN Calcd.: C, 33.04; H, 2.77; N, 7.71; Found: C, 33.05; H, 2.79; N, 7.78.

[1,4′-Bipyridine]-1,1′-diium dibromide x-hydrate: [1,4′-bipyridine]-1,1′-diium dichloride *x*-hydrate (3.12 g) was added to a Schlenk flask with a stir bar and was dissolved in concentrated HBr (9M, 10 mL). A stream of air was passed over the solution until the solution evaporated to dryness. This process was repeated three times. The solid was recovered and stored in a desiccator. The crude product was used in the synthesis of **2** without further purification (Yield: 4.10 g, 94.8%) (anh). IR (cm^{-1}): 3254 (br, m), 3049 (w), 3020 (m, mult), 2534 (v br, w), 1606 (m), 1505 (w), 1488 (w), 1468 (s), 1366 (w), 1239 (m), 1215 (m), 1168 (w), 1000 (m), 837 (s), 786 (s), 723 (m), 673 (s), 553 (w).

[1,4′-Bipyridine]-1,1′-diium tetrabromidocuprate (**2**): $CuBr_2$ (0.110 g, 0.494 mmol) was dissolved in ca. 5 mL H_2O. 1-(4′-pyridyl)-pyridinediium dibromide *x*-hydrate (0.162 g, 0.508 mmol) was dissolved in 3 mL 4.5 M HBr. The solutions were combined with stirring, giving a brownish solution. Two months later, purple crystals were isolated from solution via vacuum filtration, washed with methanol and dried mechanically (75 mg, 27%). IR (cm^{-1}): 3220 (w), 3052 (med, mult), 1630 (w), 1611 (s), 1525 (w), 1503 (med), 1485 (med), 1472 (s), 1354 (w), 1311 (w), 1279 (w), 1197 (w), 950 (w), 796 (med), 763 (s), 715 (med), 668 (vs), 646 (med), 547 (med). CHN Calcd.: C, 22.19; H, 1.86; N, 5.17; Found: C, 22.21; H, 1.75; N, 5.06.

3.2. Magnetism

The magnetizations of **1** and **2** were collected on a Quantum Design MPMS SQUID magnetometer from 0 to 50 kOe at 1.8 K, with several data points collected from 50 kOe to 0 kOe to check for hysteresis. As expected of copper(II) complexes, none was observed. The magnetic susceptibilities of **1** and **2** were collected in a 1 kOe applied field from 1.8 K to 310 K. The data were corrected for the temperature independent paramagnetism of the Cu(II) ion and the diamagnetic moment of the constituent atoms as estimated from Pascals constants [41].

3.3. Crystal Structure Data Collection, Solution and Refinement

Single crystal X-ray diffraction data for **1** and **2** were collected at 150 K with Bruker APEX2 software (APEX2-2014, Bruker AXS Inc., Madison, WI, USA) employing φ and ω scans. The data reduction and refinement of the cell constants were performed with Bruker SAINT software [42]. Absorption corrections were made via SADABS [43]. The structures were solved using SHELXS-97 [44] and refined using SHELXL-2016 [45]. The disorder in the orientation of **B1H** in **1** and **2** was treated by constraining the anisotropic displacement parameters and positions of the disordered C and N atoms to be the same value/position (C14 and N21, and C24 and N11 occupy the same coordinates). The disorder occupancies were fixed at 50% to agree with the required symmetry in the final refinement; free refinement of the occupancies gave 53(2)% (**1**)/50(2)% (**2**). Details of the X-ray data collection and refinement are shown in Table 1. The data have been deposited with the CCDC: 1967063 (**1**), 1967066 (**2**).

4. Conclusions

The compounds (**B1H**) [CuX_4] were synthesized and characterized via X-ray crystallography and magnetic studies, revealing the presence of very weak antiferromagnetic interactions in 3D between the CuX_4^{2-} units which pack in an ABAB ribbon with the counter-dication **B1H**. Despite the loss of one strong N–H hydrogen bond donor in the ribbon, these structures resemble quite closely those of related compounds such as (4,4′-bipyridinediium) [$CuCl_4$]. The disorder in the orientation of **B1H** may play an important role in the conservation of this ribbon structure. In future studies, the cation **B1H** can be modified to incorporate hydrogen bonding in different directions, modifying the crystal packing to achieve low dimensional magnetic systems with increased control. Further, the use of **B1** as a monocationic ligand is under investigation.

Supplementary Materials: The following are available online at http://www.mdpi.com/2304-6740/8/3/18/s1, Structural drawings of compound **1** (molecular unit, Figure S1; layer structure, Figure S2), overlay structure of **1** and **2** (Figure S3).

Author Contributions: Investigation, J.C.M., C.P.L., M.R. and M.M.T.; Writing—original draft, J.C.M.; Writing—review and editing, M.M.T. All authors have read and agreed to the published version of the manuscript.

Funding: The APC was funded by the Carlson School of Chemistry and Biochemistry at Clark University, Worcester, MA, USA.

Conflicts of Interest: The authors declare no conflict of interest.

References

1. Bu, R.; Xiong, Y.; Wei, X.; Li, H.; Zhang, C. Hydrogen Bonding in CHON-Containing Energetic Crystals: A Review. *Cryst. Growth Des.* **2019**, *19*, 5981–5997. [CrossRef]
2. Saha, S.; Mishra, M.K.; Reddy, C.M.; Desiraju, G.R. From Molecules to Interactions to Crystal Engineering: Mechanical Properties of Organic Solids. *Acc. Chem. Res.* **2018**, *51*, 2957–2967. [CrossRef] [PubMed]
3. Braga, D.; Grepioni, F.; Maini, L.; d'Agostino, S. From Solid-State Structure and Dynamics to Crystal Engineering. *Eur. J. Inorg. Chem.* **2018**, *2018*, 3597–3605. [CrossRef]
4. Lago, A.B.N.; Carballo, R.; Garciía-Martiínez, E.; Vaázquez-Loópez, E.M. Metal to Ligand Interactions and Hydrogen Bonding in the Design of Metallosupramolecular Compounds: Effect of pH and Aprotic Solvents on the Nature of Materials Based on Bis(4-pyridylthio)methane and Copper(II) Chloride. *Cryst. Growth Des.* **2011**, *11*, 59–68. [CrossRef]
5. Singh, Y.P.; Patel, R.N.; Singh, Y.; Choquesillo-Lazarte, D.; Butcher, R.J. Classical hydrogen bonding and stacking of chelate rings in new copper(II) complexes. *Dalton Trans.* **2017**, *46*, 2803–2820. [CrossRef] [PubMed]
6. Okazawa, A.; Ishida, T. Super–superexchange coupling through a hydrogen bond in a linear copper(II) complex, [Cu(LH)(L)]·BF4·2H_2O (LH = *N*-tert-butyl-*N*-2-pyridylhydroxylamine). *Chem. Phys. Lett.* **2009**, *480*, 198–202. [CrossRef]

7. Manson, J.L.; Schlueter, J.A.; Funk, K.A.; Southerland, H.I.; Twamley, B.; Lancaster, T.; Blundell, S.J.; Baker, P.J.; Pratt, F.L.; Singleton, J.; et al. Strong H···F Hydrogen Bonds as Synthons in Polymeric Quantum Magnets: Structural, Magnetic, and Theoretical Characterization of $[Cu(HF_2)(pyrazine)_2]SbF_6$, $[Cu_2F(HF)(HF_2)(pyrazine)](SbF_6)_2$, and $[CuAg(H_3F_4)(pyrazine)_5](SbF_6)_2$. *J. Am. Chem. Soc.* **2009**, *131*, 6733–6747. [CrossRef]
8. Tang, J.; Costa, J.S.; Golobic, A.; Kozlevcar, B.; Robertazzi, A.; Vargiu, A.V.; Gamez, P.; Reedijk, J. Magnetic coupling between copper(II) ions mediated by hydrogen-bonded (neutral) water molecules. *Inorg. Chem.* **2009**, *48*, 5473–5479. [CrossRef]
9. Goodgame, D.M.L.; Grachvogel, D.A.; Williams, D.J. Combination of weak covalent, hydrogen bonding, and Ag$\cdots\pi$ interactions in the formation of a 3D porous network $Ag(pypd)_2(ClO_4)\cdot CH_2Cl_2$ by the ambidentate ligand 1-(4′-pyridyl)pyridin-4-one. *J. Chem. Soc. Dalton Trans.* **2002**, *11*, 2259–2260. [CrossRef]
10. Kumar, D.K.; Ballabh, A.; Jose, D.A.; Dastidar, P.; Das, A. How Robust Is the N–H···Cl_2-Cu Synthon? Crystal Structures of Some Perchlorocuprates. *Crys. Growth Des.* **2005**, *5*, 651–660.
11. Willett, R.D.; Butcher, R.E.; Landee, C.P.; Twamley, B. Two halide exchange in copper(II) halide dimers: (4,4′-Bipyridinium)$Cu_2Cl_{6-x}Br_x$. *Polyhedron* **2006**, *25*, 2093–2100. [CrossRef]
12. Yahsi, Y.; Gungor, E.; Kara, H. Chlorometallate-Pyridinium Boronic Acid Salts for Crystal Engineering: Synthesis of One-, Two-, and Three-Dimensional Hydrogen Bond Networks. *Cryst. Growth Des.* **2015**, *15*, 2652–2660. [CrossRef]
13. Dgachi, S.; Ben Salah, A.M.; Turnbull, M.M.; Bataille, T.; Naili, H. Investigations on $(C_6H_9N_2)_2[M^{II}Br_4]$ halogenometallate complexes with MII = Co, Cu and Zn: Crystal structure, thermal behavior and magnetic properties. *J. Alloys Comps.* **2017**, *726*, 315–322. [CrossRef]
14. Solomon, B.L.; Landee, C.P.; Turnbull, M.M.; Wikaira, J.L. Copper(II) complexes of 2-amino-5-chloro-3-fluoropyridine: Syntheses and magnetic properties of $(3,5\text{-FCAP})_2CuX_2$ and $(3,5\text{-FCAPH})_2CuX_4$. *J. Coord. Chem.* **2014**, *67*, 3953–3971. [CrossRef]
15. Hong, T.; Gvasaliya, S.N.; Herringer, S.N.; Turnbull, M.M.; Landee, C.P.; Regnault, L.-P.; Boehm, M.; Zheludev, A. Dynamics of the two-dimensional S = 1/2 dimer system $(C_5H_6N_2F)2CuCl_4$. *Phy. Rev. B* **2011**, *83*, 052401. [CrossRef]
16. Tremelling, G.W.; Foxman, B.M.; Landee, C.P.; Turnbull, M.M.; Willett, R.D. Transition metal complexes of 2-amino-3,5-dihalopyridines: Syntheses, structures and magnetic properties of $(3,5\text{-diCAPH})_2CuX_4$ and $(3,5\text{-diBAPH})_2CuX_4$. *Dalton Trans.* **2009**, *47*, 10518–10526. [CrossRef]
17. Deumal, M.; Giorgi, G.; Robb, M.A.; Turnbull, M.M.; Landee, C.P.; Novoa, J.J. The mechanism of magnetic interaction in spin-ladder molecular magnets: A first-principles, bottom-up, theoretical study of the magnetism in the two-legged spin-ladder bis(2-amino-5-nitropyridinium) tetrabromocuprate monohydrate. *Eur. J. Inorg. Chem.* **2005**, *2005*, 4697–4706. [CrossRef]
18. Woodward, F.M.; Albrecht, A.S.; Wynn, C.M.; Landee, C.P.; Turnbull, M.M. Two-dimensional S = 1/2 Heisenberg antiferromagnets: Synthesis, structure, and magnetic properties. *Phys. Rev. B* **2002**, *65*, 144412. [CrossRef]
19. Al Damen, M.A.; Haddad, S.F. The nonclassical noncovalent interactions control: A case study of the crystal structure of 3,5-dibromo-2-amino-4,6-dimethylpyridinium tetrahalocuprate $[3,5\text{-DBr-2-A-4,6-DMPH}]_2CuX_4$ (X = Cl, and Br). *J. Mol. Struct.* **2011**, *985*, 27–33. [CrossRef]
20. Gong, J.; Chen, G.; Ni, S.F.; Zhang, Y.Y.; Wang, H.B. Bis(2-amino-6-methylpyridinium) tetrachloridocuprate(II). *Acta Crystallogr. Sect. E* **2009**, *65*, m1661–m1662. [CrossRef]
21. Kovalchukova, O.V.; Palkina, K.K.; Strashnova, S.B.; Zaitsev, B.E. Synthesis, structure, geometrical, and spectral characteristics of the $(HLn)_2[CuCl_4]$ complexes. Crystal and molecular structure of bis(2-methylimidazolium) tetrachlorocuprate(II). *Russ. J. Coord. Chem.* **2008**, *34*, 830–835. [CrossRef]
22. Haddad, S.F.; AlDamen, M.A.; Willett, R.D. The role of non-classical supramolecular interactions in the structures of 2-amino-4,6-dimethylpyridinium tetrahalocuprate(II) salts. *Inorg. Chim. Acta* **2006**, *359*, 424–432. [CrossRef]
23. Boutchard, C.L.; Hitchman, M.A.; Skelton, B.W.; White, A.H. Crystal structure and electronic spectrum of the distorted tetrahedral $CuCl_4^{2-}$ ion in bis(2-aminopyridinium) tetrachlorocuprate(II) and comparison with the tetragonally elongated octahedral complex bis(2-aminopyrimidinium)tetrachlorocopper(II). *Aust. J. Chem.* **1995**, *48*, 771–781. [CrossRef]

24. Place, H.; Willett, R.D. Structure of catalytically related species involving copper(II) halides. III. 2-Amino-5-bromo-3-methylpyridinium 2-amino-3-methylpyridinium tetrabromocuprate(II). *Acta Crystallogr. Sect. C* **1987**, *43*, 1497–1500. [CrossRef]
25. Walha, S.; Naili, H.; Yahyaoui, S.; Ali, B.F.; Turnbull, M.M.; Mhiri, T.; Ng, S.W. Three-Dimensional Network Polymeric Structure of (2-Amino-5-ammoniopyridinium)[$CuCl_4$]: Crystal Supramolecularity and Magnetic Properties. *J. Supercond. Nov. Magn.* **2013**, *26*, 437–442. [CrossRef]
26. Lee, Y.-M.; Park, S.-M.; Kang, S.K.; Kim, Y.-I.; Choi, S.-N. Crystal Structures and Magnetic Properties of Sparteinium Tetrahalocuprate Monohydrate Compounds. *Bull. Kor. Chem. Soc.* **2004**, *25*, 823–828.
27. Wikaira, J.L.; Butcher, R.J.; Kersen, Ü.; Turnbull, M.M. Magnetic properties of 4,4′-bipiperidinediium tetrahalocuprates: Crystal structures of 4,4′-bipiperidinediium tetrabromocuprate(II) monohydrate and bis(4,4′-bipiperidinediium) hexabromodicuprate(I). *J. Coord. Chem.* **2015**, *69*, 57–71. [CrossRef]
28. Turnbull, M.M.; Landee, C.P.; Wells, B.M. Magnetic exchange interactions in tetrabromocuprate compounds. *Coord. Chem. Rev.* **2005**, *249*, 2567–2576. [CrossRef]
29. Yang, L.; Powell, D.R.; Houser, R.P. Structural variation in copper(I) complexes with pyridylmethylamide ligands: Structural analysis with a new four-coordinate geometry index, τ4. *Dalton Trans.* **2007**, *9*, 955–964. [CrossRef]
30. Brenčič, J.V.; Čeh, B.; Leban, I. Structure of 1-(4-pyridyl)pyridinium trans-tetrachlorodi(pyridine)molybdate(III). *Acta Crystallogr. Sect. C* **1989**, *45*, 1144–1146. [CrossRef]
31. Brenčič, J.V.; Čeh, B.; Leban, I. Preparation, Chemical, and Structural Characterization of Some Molybdenum(III) and Tungsten(III) Coordination Compounds Containing 1-(4-pyridyl)pyridinium Cation. *Z. Anorg. Allg. Chem.* **1988**, *565*, 163–170. [CrossRef]
32. Goodgame, D.M.L.; Grachvogel, D.A.; White, A.J.P.; Williams, D.J. Diverse polymeric metal complexes formed by the ambidentate ligand 1-(4′-pyridyl)pyridin-4-one. *Inorg. Chim. Acta* **2003**, *348*, 187–193. [CrossRef]
33. Angeloni, A.; Crawford, P.C.; Orpen, A.G.; Podesta, T.J.; Shore, B.J. Does Hydrogen Bonding Matter in Crystal Engineering? Crystal Structures of Salts of Isomeric Ions. *Chem. Eur. J.* **2004**, *10*, 3783–3791. [CrossRef] [PubMed]
34. Gorelsky, S.I.; Ilyukhin, A.B.; Kholin, P.V.; Kotov, V.Y.; Lokshin, B.V.; Sapoletova, N.V. Dihydrohexacyanoferrates of *N*-heterocyclic cations. *Inorg. Chim. Acta* **2007**, *360*, 2573–2582. [CrossRef]
35. Li, L.; Turnbull, M.M.; Landee, C.P.; Jornet, J.; Deumal, M.; Novoa, J.J.; Wikaira, J.L. Synthesis, structure and magnetic behavior of bis(2-amino-5-fluoropyridinium) tetrachlorocuprate(II). *Inorg. Chem.* **2007**, *46*, 11254–11265. [CrossRef]
36. Landee, C.P.; Turnbull, M.M. A gentle introduction to magnetism: Units, fields, theory, and experiment. *J. Coord. Chem.* **2014**, *67*, 375–439. [CrossRef]
37. Stoll, S.; Schweiger, A. EasySpin, a comprehensive software package for spectral simulation and analysis in EPR. *J. Magn. Reson.* **2006**, *178*, 42–55. [CrossRef]
38. Farra, R.; Thiel, K.; Winter, A.; Klamroth, T.; Pöppl, A.; Kelling, A.; Schilde, U.; Taubert, A.; Strauch, P. Tetrahalidocuprates(II)—Structure and EPR spectroscopy. Part 1: Tetrabromidocuprates(II). *New J. Chem.* **2011**, *35*, 2793. [CrossRef]
39. Willett, R.D.; Wong, R.J. Experimental Evidence for Phonon Modulation of Antisymmetric Exchange from the Temperature Dependence of EPR Linewidths in $(RNH_3)_2CuX_4$ Salts. *J. Magn. Reson.* **1981**, *42*, 446–452. [CrossRef]
40. Monroe, J.C.; Rademeyer, M.; Turnbull, M.M. Compounds of pyridylpyridones. In preparation.
41. Carlin, R.L. *Magnetochemistry*; Springer: Berlin/Heidelberg, Germany, 1986.
42. Bruker. *SAINT-2012*, Bruker AXS Inc.: Madison, Wisconsin, USA, 2012.
43. Bruker SADABS. *Version 2014/5*, Bruker AXS Inc.: Madison, WI, USA.
44. Sheldrick, G.M. A short history of SHELX. *Acta Cryst. A* **2008**, *64*, 112–122. [CrossRef]
45. Sheldrick, G.M. Crystal structure refinement with SHELXL. *Acta Cryst.* **2015**, *71*, 3–8.